

Multidimensional De Novo Design Reveals 5-HT_{2B} Receptor-Selective Ligands**

Tiago Rodrigues, Nadine Hauser, Daniel Reker, Michael Reutlinger, Tiffany Wunderlin, Jacques Hamon, Guido Koch, and Gisbert Schneider*

Abstract: We report a multi-objective de novo design study driven by synthetic tractability and aimed at the prioritization of computer-generated 5-HT_{2B} receptor ligands with accurately predicted target-binding affinities. Relying on quantitative bioactivity models we designed and synthesized structurally novel, selective, nanomolar, and ligand-efficient 5-HT_{2B} modulators with sustained cell-based effects. Our results suggest that seamless amalgamation of computational activity prediction and molecular design with microfluidics-assisted synthesis enables the swift generation of small molecules with the desired polypharmacology.

Computational molecular design methods offer an opportunity to promptly combat the perceived dearth of innovation in drug discovery.^[1] In particular, de novo design and prediction of polypharmacology networks are maturing technologies for productive lead identification in chemical biology and medicinal chemistry.^[1a,2] However, de novo design has only been applied on a limited scale.^[3] Here, we present a pioneering large-scale de novo design study with swift design–synthesis–bioassay cycles, aimed at the discovery of new chemical entities (NCEs) engaging the human serotonin 2B (5-HT_{2B}) receptor. By combining the computational design and quantitative affinity prediction with microfluidics synthesis,^[4] the multi-objective NCE prioritization afforded structurally novel, nanomolar-potent, and ligand-efficient compounds ($LE > 0.34$) with G protein-coupled receptor (GPCR) selectivity in functional cell-based assays. Our findings not only corroborate de novo design and machine-learning methods as prime utensils for exploring uncharted chemical space, but also suggest that the amalga-

mation of such computational tools with the automated synthesis of designer molecules may be suitable for rapidly obtaining NCEs with the desired target engagement.

We focused on the 5-HT_{2B} receptor as a challenge for this proof-of-concept study. Antagonistic small-molecular effectors may serve as probes to study the pathophysiology of migraine, pulmonary hypertension, and chronic heart failure.^[5] On the other hand, engagement of 5-HT_{2B} receptors by small molecule agonists results in cardiac valvulopathy, a severe adverse drug reaction that leads to chemotype deprioritization.^[6] Consequently, reports of selective ligands that may yield therapeutic benefits are rare, and clinical trials with 5-HT_{2B} receptor antagonist PGN-1164 were stopped due to unsuitable pharmacokinetics.^[5d] Moreover, the rational design of 5-HT_{2B} selectivity remains arduous.^[2c] Building on our previous work using Gaussian process (GP) models for designing NCEs^[7] and de-orphaning a focused combinatorial library^[8] we envisaged that such a computational approach, coupled to microfluidics-assisted syntheses, could efficiently afford 5-HT_{2B} ligands.

We employed the MAntA molecular design software^[7] implementing the reductive amination as a privileged tool reaction for adaptive building block prioritization to obtain 5-HT_{2B}-selective ligands. Using both CATS2^[9] pharmacophores and Morgan substructure fingerprints,^[10] the machine-learning algorithm generated 5774 candidate amines, from which we selected **1–4** for synthesis and biochemical profiling [Table 1, Figure 1 A, Supporting Information (SI)], based on the predicted 5-HT_{2B} selectivity over 5-HT_{2A/C}. To enable rapid design cycles, our efforts initially focused on developing

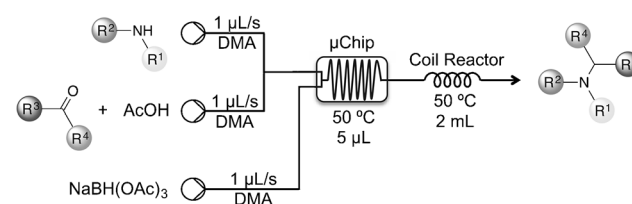


Figure 1. Microfluidics-assisted synthesis of amines.

a scalable and robust reductive amination process in flow.^[11] We used an automated Cetoni neMESYS microfluidic system equipped with low-pressure, pulsation-free syringe pumps. The platform included a 3-2-way solenoid valve, a 5 µL borosilicate DeanFlow microreactor chip as primary reactor, and a coil reactor (2 mL) as secondary reactor (Figure 1). Stock solutions of all reaction components were prepared in dimethylacetamide (DMA) and the reaction was quenched

[*] Dr. T. Rodrigues,^[‡] N. Hauser,^[‡] D. Reker, Dr. M. Reutlinger, Prof. Dr. G. Schneider
Department of Chemistry and Applied Biosciences
Swiss Federal Institute of Technology (ETH)
Vladimir-Prelog-Weg 4, 8093 Zurich (Switzerland)
E-mail: gisbert.schneider@pharma.ethz.ch
T. Wunderlin, Dr. J. Hamon, Dr. G. Koch
Novartis Institutes for BioMedical Research (NIBR)
Novartis AG, 4056 Basel (Switzerland)

[‡] These authors contributed equally to this work.

[**] N.H. and T.R. performed organic syntheses. D.R. and M.R. contributed computational tools and performed in silico experiments together with N.H. and T.R. T.W., J.H., and G.K. contributed binding assays. All authors analyzed and discussed data. T.R. and G.S. designed the study and wrote the manuscript with feedback from the remaining authors.

Supporting information for this article is available on the WWW under <http://dx.doi.org/10.1002/anie.201410201>.

Table 1: MAnTA de novo designed molecules **1–4** and nearest neighbors from the ChEMBL^[14] training data.

MAnTA designs		IC ₅₀ ± SD [nM] ^[a]	Nearest neighbors from training data ID ^[b]	Structure	Structural similarity ^[c]	pK _i
Cpd.	Structure					
1		886 ± 314	196514		0.32	9.0 ^[15]
2		3570 ± 40	1214961		0.57	8.0 ^[16]
3		7109 ± 1722	209324		0.37	7.3 ^[17]
4		1051 ± 61	196514		0.31	9.0 ^[15]

[a] Functional cell-based assay (IP1 quantification by HTRF detection, see SI); [b] “ChEMBL” prefix omitted from ID; [c] Tanimoto similarity index calculated with Morgan substructure fingerprints (radius = 4, 2048 bit). SD: standard deviation ($n = 3$).

with NaHCO₃ following a residence time of ca. 10 min (SI). Whereas **1–3** could be acquired in flow, **4** was obtained in batch due to low solubility of the building blocks in DMA. With screening compounds **1–4** in hand, we performed radioligand displacement assays, confirming the usefulness of the predicted binding affinities (*pAffinity*) (5-HT_{2B} *pAffinity* ≥ 7.0, experimental *pK_i* ≥ 6.0, Figure 2A). The majority of the *pAffinity* estimates were in agreement with the measured data, taking into account the GP models’ background error (*pK_i* = *pAffinity* ± 0.8; Figure 2A). Furthermore, all compounds showed moderate antagonistic behavior in a functional cell-based assay (Table 1), and good ligand efficiency (*LE* ≥ 0.35, Figure 2A). Under dynamic light scattering none of the compounds presented measurable colloidal aggregation at a concentration of 100 μM that could equate unspecific binding and artefacts when probing for antagonistic behavior in GPCRs.^[12]

We further screened compounds **1–4** in functional assays at 10 μM, to assess the scope of the predictive models. As tool GPCRs, we selected 5-HT_{2A} and related off-targets (adrenergic α_{1A} and dopamine D₂ receptors,^[2c,6,13] Figure 2B). The potent in vitro effects and high ligand efficiencies of the de novo designed compounds, the moderate selectivity (Table 1 and Figure 2B,C) and general scaffold innovation (SciFinder, www.scifinder.org) compared to the nearest neighbors in ChEMBL (substructure-based Tanimoto similarity ~0.4), suggest that **1–3** may serve as 5-HT_{2B}-selective leads for future development. The LiSARD^[18] software generates interactive graphics by computing structure–activity relationship landscapes that may serve as roadmaps for molecular design and compound prioritization. For this study, the overlapping preferred design areas for 5-HT_{2A–C} receptors certified the difficulty of simultaneously obtaining potent and selective 5-HT_{2B}-targeting NCEs (Figure 2C). Notwithstanding these promising preliminary results obtained with

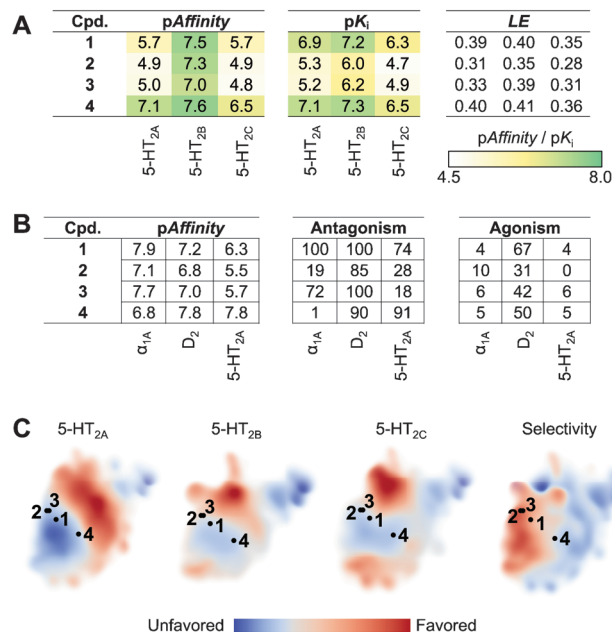


Figure 2. A) Predicted variance-corrected affinity (*pAffinity*) and experimental *pK_i* values obtained for **1–4** through radioligand displacement assays against 5-HT_{2A–C}. Ligand efficiency *LE* = (−1.4 log *K_i*)/number heavy atoms. B) Cell-based functional effects (%antagonism and agonism) of **1–4** against selected off-targets (10 μM, $n = 2$). Note: Full details on controls are provided in the SI. C) LiSARD^[18] landscapes (CATS2 pharmacophore descriptors) for 5-HT_{2A–C} receptor binding and 5-HT_{2B} selectivity over 5-HT_{2A/C}. Landscapes were computed from available ChEMBL version 16 affinity data and **1–4**: 3269 (5-HT_{2A}), 1719 (5-HT_{2B}), and 3307 (5-HT_{2C}) small molecules, totaling 4137 unique entities.

MAnTA, we recognized that engagement of the dopamine D₂ receptor by **1–4** would constitute a significant liability (Figure 2B). As a consequence, we envisaged that increasing the

scaffold diversity of the computationally designed chemotypes might help us find molecules with improved 5-HT_{2B} selectivity. Therefore, we employed the de novo design software DOGS^[19] coupled to the GP prediction models to generate NCEs, taking 239 GPCR-targeting and FDA-approved small molecules as design templates (GPCR SARfari, <http://www.ebi.ac.uk>). We aimed at increasing the framework diversity of de novo-designed molecules by expanding the search space with up to 58 tractable reaction types for stepwise fragment growing.^[19] Furthermore, we employed a large template set (SARfari), as target promiscuity is common among GPCR ligands.^[2c] From the DOGS runs we obtained 111 854 unique, synthetically accessible and GPCR-ligand-like designs. A total of 25 363 Murcko scaffolds with profound dissimilarity to the design templates and annotated high-affinity 5-HT_{2B} ligands in ChEMBL (average structural Tanimoto similarity = 0.13 ± 0.07 and 0.17 ± 0.04, respectively) highlight the scaffold-hopping capabilities and intrinsic explorative nature of the DOGS algorithm.

We subjected all designed NCEs to the PAINS^[20] and ADMET^[21] filters to eliminate potentially undesirable small molecules and scored the remaining 78 468 designs with the GP target prediction models. In line with previous findings in which ca. 30% of the Novartis corporate compound library binds to 5-HT_{2B} at 10 μM,^[13] the computationally designed molecules presented an average pAffinity value of 5.0 ± 0.6. For the training data we computed an average pAffinity value of 5.1 ± 0.5, suggesting no bias in the design and scoring algorithms towards 5-HT_{2B} ligands over other GPCRs. We selected compounds **5–8** for subsequent synthesis according to either pAffinity and/or GPCR-panel selectivity criteria. Although no 5-HT_{2B} selectivity was forecast for **5** (Figure 3A), we chose it because of its chemical similarity to aripiprazole^[24] (Tanimoto similarity = 0.51) and its predicted 5-HT_{2B} binding affinity (pAffinity = 6.8). Analogously to its template (Table 2) and as predicted by the GP models, compound **5** showed binding affinity for 5-HT_{2A-B} (Figure 3A). Our results suggest the importance of structural features in aripiprazole for potent 5-HT_{2B} binding and overall 5-HT₂ receptor subtype selectivity. In an orthogonal assay, **5** showed a strong 5-HT_{2B} antagonistic effect (IC₅₀ = 225 ± 26 nM; Figure 3B), fully corroborating receptor binding. The remaining pooled designs were analyzed for potential 5-HT_{2B} selectivity over other GPCRs and hERG. Although no design revealed clear predicted selectivity over the 5-HT_{2A/C} and D₂ receptors simultaneously, the engagement of 5-HT_{2C} is apparently uncorrelated with known adverse drug reactions.

Consequently, we prioritized compounds **6–8** based on GPCR panel selectivity, including the 5-HT_{2A} and D₂ receptors (Figure 3A and SI). Compounds **6** and **7** were designed from the low-affinity 5-HT_{2B} ligands rizatriptan and metaminalol, respectively. Molecule **6** had already been disclosed as a 5-HT_{2B} receptor agonist,^[25] but its selectivity over the dopamine D₂ receptor remained unknown. Although limited utility as a drug lead may be foreseen for **6**, due to 5-HT_{2B} agonism, the herein experimentally confirmed potent functional effect (EC₅₀ = 18 ± 3 nM; Figure 2B) and GPCR panel selectivity (Figure 3C, SI) may still warrant high value as a chemical probe. A two-step synthetic route afforded **7**. Despite its excellent overall selectivity (Figure 3C), the moderate 5-HT_{2B} binding affinity (K_i = 1700 ± 25 nM; Figure 3A) was translated into an undesired partial agonistic effect (EC₅₀ = 2365 ± 243 nM; Figure 3B). Irrespective of the functional activity of the profiled ligands, the computer-assisted design method (DOGS) fulfilled our primary goal of designing GPCR-tailored ligands with accurately predicted selectivity profiles. Compound retrieval by library enumeration and similarity searching would probably have failed to identify **6–7** as screening candidates due to their low structural similarity to the design templates as well as the ChEMBL training data (Table 2). Our final focus was on the piperazine derivative **8**, which we acquired in flow. Binding assessment against the 5-HT₂ receptor panel revealed selectivity toward 5-HT_{2B} (K_i = 251 ± 0.02 nM, LE = 0.42; 5-HT_{2A}: K_i = 3383 ± 1100 nM; 5-HT_{2C}: K_i = 18 100 ± 1570 nM), a potent antagonistic effect in vitro (IC₅₀ = 611 ± 240 nM, Figure 3B) and functional selectivity against a panel of GPCR off-targets and the hERG cardiac potassium channel (Figure 3C). These results are important taking into account that **8** presented no

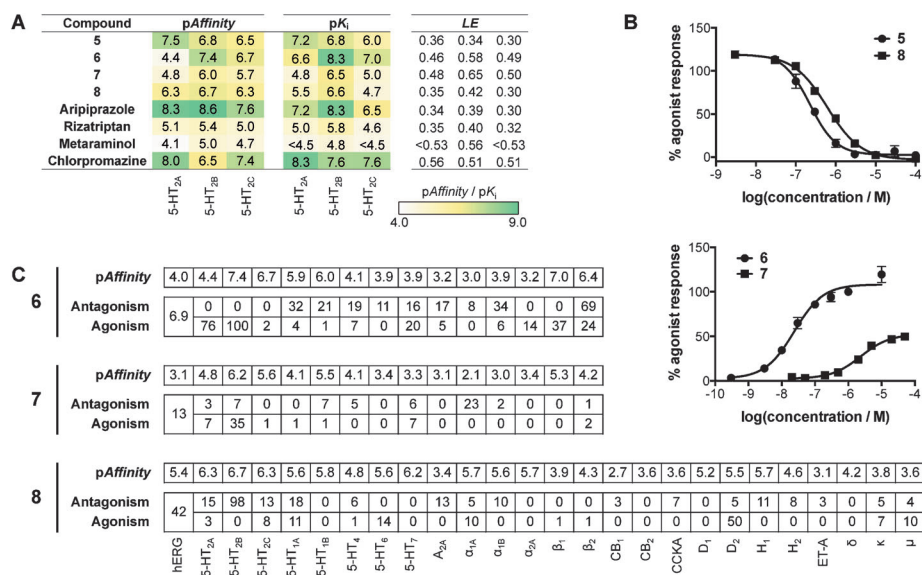


Figure 3. A) Predicted affinity (pAffinity) and experimental pK_i values obtained for **5–8** and template structures through radioligand assays against 5-HT_{2A-C}. Ligand efficiency LE = (−1.4 log K_i)/number heavy atoms. B) Cell-based

Table 2: DOGS de novo designed molecules **5–8** and nearest neighbors from the ChEMBL training data.

DOGS designs		Template	Structural similarity ^[a]	Nearest neighbors from training data ID ^[b]	Structure	Structural similarity ^[a]	p <i>K</i> _i
Cpd.	Structure						
5			0.51	1112		0.51	8.9 ^[15]
		aripiprazole					
6			0.16	1255834		1.0	8.6 ^[22]
		rizatriptan					
7			0.16	402794		0.29	< 5.0
		metaraminol					
8			0.16	7257		0.26	7.3 ^[23]
		chlorpromazine					

[a] Tanimoto similarity index calculated with Morgan substructure fingerprints (radius = 4, 2048 bit); [b] "ChEMBL" prefix omitted from ID.

measurable colloidal aggregation at concentrations at least 200-fold higher than the relevant bioactive concentration. Furthermore, **8** presents high water solubility (kinetic solubility > 80 $\mu\text{g mL}^{-1}$) and can be acquired in one synthetic step. Peculiarly, the design template of **8**, chlorpromazine, revealed complete absence of 5-HT₂ receptor panel selectivity, and the nearest neighbor in the training data (ChEMBL7257, Table 2) is a 5-HT_{2B} agonist with similar receptor affinity as **8**.^[23]

Although there are more potent and 5-HT_{2B} receptor-selective antagonists described in the literature, for example, RS-127445^[26] and PRX-08066,^[27] we consider the design of **8** a successful outcome of this proof-of-concept study aiming at target-panel selectivity. The compound was readily obtained without the need for high-throughput screening or lengthy hit optimization. The discovery platform described herein is widely applicable to quickly identify starting points for other GPCRs and drug target families, provided that templates for de novo design are available. Our GP models currently encompass several hundred human drug targets. Additional affinity prediction models should become available with publicly accessible database updates. The results of this study suggest a feasible solution for fast fragment-based de novo design of NCEs with accurately predicted designer polypharmacological or selectivity profiles. Together with the polygenic nature of several diseases, such platforms may be suited to economically prototype efficacious tools for personalized medicine.^[28] The results obtained validate the combination of machine-learning methods with automated chemical synthesis and fast bioassay turnover as a general approach for rapid hit and lead discovery.

Received: October 20, 2014

Revised: October 30, 2014

Published online: December 4, 2014

Keywords: computer-assisted molecular design · drug discovery · GPCR · microfluidics · organic synthesis

- [1] a) T. Rodrigues, G. Schneider, *Synlett* **2014**, 25, 170–178; b) Y. L. Bennani, *Drug Discovery Today* **2011**, 16, 779–792.
- [2] a) A. L. Hopkins, *Nat. Chem. Biol.* **2008**, 4, 682–690; b) J. Besnard, G. F. Ruda, V. Setola, K. Abecassis, R. M. Rodriguez, X. P. Huang, S. Norval, M. F. Sassano, A. I. Shin, L. A. Webster, F. R. Simeons, L. Stojanovski, A. Prat, N. G. Seidah, D. B. Constam, G. R. Bickerton, K. D. Read, W. C. Wetsel, I. H. Gilbert, B. L. Roth, A. L. Hopkins, *Nature* **2012**, 492, 215–220; c) H. Lin, M. F. Sassano, B. L. Roth, B. K. Shoichet, *Nat. Methods* **2013**, 10, 140–146; d) E. Lounkine, M. J. Keiser, S. Whitebread, D. Mikhailov, J. Hamon, J. L. Jenkins, P. Lavan, E. Weber, A. K. Doak, S. Cote, B. K. Shoichet, L. Urban, *Nature* **2012**, 486, 361–367; e) M. J. Keiser, B. L. Roth, B. N. Armbruster, P. Ernsberger, J. J. Irwin, B. K. Shoichet, *Nat. Biotechnol.* **2007**, 25, 197–206; f) D. Reker, T. Rodrigues, P. Schneider, G. Schneider, *Proc. Natl. Acad. Sci. USA* **2014**, 111, 4067–4072.
- [3] a) T. Rodrigues, T. Kudoh, F. Roudnicki, Y. F. Lim, Y.-C. Lin, C. P. Koch, M. Seno, M. Detmar, G. Schneider, *Angew. Chem. Int. Ed.* **2013**, 52, 10006–10009; *Angew. Chem.* **2013**, 125, 10190–10193; b) B. Spänkuch, S. Keppner, L. Lange, T. Rodrigues, H. Zettl, C. P. Koch, M. Reutlinger, M. Hartenfeller, P. Schneider, G. Schneider, *Angew. Chem. Int. Ed.* **2013**, 52, 4676–4681; *Angew. Chem.* **2013**, 125, 4774–4779; c) T. Rodrigues, F. Roudnicki, C. P. Koch, T. Kudoh, D. Reker, M. Detmar, G. Schneider, *Chem. Sci.* **2013**, 4, 1229–1233.
- [4] a) T. Rodrigues, P. Schneider, G. Schneider, *Angew. Chem. Int. Ed.* **2014**, 53, 5750–5758; *Angew. Chem.* **2014**, 126, 5858–5866; b) K. S. Elvira, X. Casadevall i Solvas, R. C. Wootton, A. J. deMello, *Nat. Chem.* **2013**, 5, 905–915.
- [5] a) M. Berger, J. A. Gray, B. L. Roth, *Annu. Rev. Med.* **2009**, 60, 355–366; b) N. Moss, Y. Choi, D. Cogan, A. Flegg, A. Kahrs, P. Loke, O. Meyn, R. Nagaraja, S. Napier, A. Parker, J. T. Peterson, P. Ramsden, C. Sarko, D. Skow, J. Tomlinson, H. Tye, M. Whitaker, *Bioorg. Med. Chem. Lett.* **2009**, 19, 2206–2210; c) Y. J. Kwon, S. Saubern, J. M. Macdonald, X. P. Huang, V. Setola, B. L.

- Roth, *Bioorg. Med. Chem. Lett.* **2010**, 20, 5488–5490; d) *Encyclopedia of Molecular Pharmacology*, 2nd ed. (Eds.: S. Offermanns, W. Rosenthal), Springer, Heidelberg, **2008**, p. 1125.
- [6] J. Hamon, S. Whitebread, V. Techer-Etienne, H. Le Coq, K. Azzaoui, L. Urban, *Future Med. Chem.* **2009**, 1, 645–665.
- [7] M. Reutlinger, T. Rodrigues, P. Schneider, G. Schneider, *Angew. Chem. Int. Ed.* **2014**, 53, 4244–4248; *Angew. Chem.* **2014**, 126, 4330–4334.
- [8] M. Reutlinger, T. Rodrigues, P. Schneider, G. Schneider, *Angew. Chem. Int. Ed.* **2014**, 53, 582–585; *Angew. Chem.* **2014**, 126, 593–596.
- [9] M. Reutlinger, C. P. Koch, D. Reker, N. Todoroff, P. Schneider, T. Rodrigues, G. Schneider, *Mol. Inf.* **2013**, 32, 133–138.
- [10] D. Rogers, M. Hahn, *J. Chem. Inf. Model.* **2010**, 50, 742–754.
- [11] J. E. Hochlowski, P. A. Searle, N. P. Tu, J. Y. Pan, S. G. Spanton, S. W. Djuric, *J. Flow Chem.* **2011**, 2, 56–61.
- [12] M. F. Sassano, A. K. Doak, B. L. Roth, B. K. Shoichet, *J. Med. Chem.* **2013**, 56, 2406–2414.
- [13] J. Bowes, A. J. Brown, J. Hamon, W. Jarolimek, A. Sridhar, G. Waldron, S. Whitebread, *Nat. Rev. Drug Discovery* **2012**, 11, 909–922.
- [14] A. Gaulton, L. J. Bellis, A. P. Bento, J. Chambers, M. Davies, A. Hersey, Y. Light, S. McGlinchey, D. Michalovich, B. Al-Lazikani, J. P. Overington, *Nucleic Acids Res.* **2012**, 40, D1100–D1107.
- [15] J. H. Lange, J. H. Reinders, J. T. Tolboom, J. C. Glennon, H. K. Coolen, C. G. Kruse, *J. Med. Chem.* **2007**, 50, 5103–5108.
- [16] I. A. Moussa, S. D. Banister, C. Beinart, N. Giboureau, A. J. Reynolds, M. Kassiou, *J. Med. Chem.* **2010**, 53, 6228–6239.
- [17] O. M. Becker, D. S. Dhanoa, Y. Marantz, D. Chen, S. Shacham, S. Cheruku, A. Heifetz, P. Mohanty, M. Fichman, A. Sharadendu, R. Nudelman, M. Kauffman, S. Noiman, *J. Med. Chem.* **2006**, 49, 3116–3135.
- [18] M. Reutlinger, W. Guba, R. E. Martin, A. I. Alanine, T. Hoffmann, A. Klenner, J. A. Hiss, P. Schneider, G. Schneider, *Angew. Chem. Int. Ed.* **2011**, 50, 11633–11636; *Angew. Chem.* **2011**, 123, 11837–11840.
- [19] M. Hartenfeller, H. Zettl, M. Walter, M. Rupp, F. Reisen, E. Proschak, S. Weggen, H. Stark, G. Schneider, *PLoS Comput. Biol.* **2012**, 8, e1002380.
- [20] J. B. Baell, G. A. Holloway, *J. Med. Chem.* **2010**, 53, 2719–2740.
- [21] D. Lagorce, O. Sperandio, H. Galons, M. A. Miteva, B. O. Villoutreix, *BMC Bioinf.* **2008**, 9, 396.
- [22] S. P. Alexander, A. Mathie, J. A. Peters, *Br. J. Pharmacol.* **2009**, 158, S1–S254.
- [23] J. A. May, A. P. Dantanarayana, P. W. Zinke, M. A. McLaughlin, N. A. Sharif, *J. Med. Chem.* **2006**, 49, 318–328.
- [24] J. D. Urban, G. A. Vargas, M. von Zastrow, R. B. Mailman, *Neuropsychopharmacology* **2007**, 32, 67–77.
- [25] S. P. Alexander, A. Mathie, J. A. Peters, *Br. J. Pharmacol.* **2011**, 164, S1–S324.
- [26] D. W. Bonhaus, L. A. Flippin, R. J. Greenhouse, S. Jaime, C. Rocha, M. Dawson, K. Van Natta, L. K. Chang, T. Pulido-Rios, A. Webber, E. Leung, R. M. Eglén, G. R. Martin, *Br. J. Pharmacol.* **1999**, 127, 1075–1082.
- [27] S. L. Porvasnik, S. Germain, J. Embury, K. S. Gannon, V. Jacques, J. Murray, B. J. Byrne, S. Shacham, R. Al-Mousily, *J. Pharmacol. Exp. Ther.* **2010**, 334, 364–372.
- [28] W. E. Evans, J. A. Johnson, *Annu. Rev. Genomics Hum. Genet.* **2001**, 2, 9–39.